

Synthesis and Reactivity of 4,4-Dialkoxy-BODIPYs: An Experimental and Computational Study

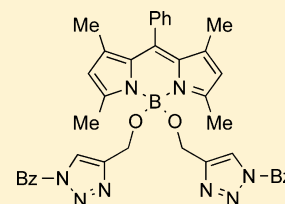
Alex L. Nguyen,[†] Petia Bobadova-Parvanova,[‡] Melissa Hopfinger,[‡] Frank R. Fronczek,[†] Kevin M. Smith,[†] and M. Graça H. Vicente^{*†}

[†]Department of Chemistry, Louisiana State University, Baton Rouge, Louisiana 70803, United States

[‡]Department of Chemistry, Rockhurst University, Kansas City, Missouri 64110, United States

S Supporting Information

ABSTRACT: A series of boron-disubstituted *O*-BODIPYs were synthesized, and their structures and spectroscopic properties were investigated using both computational and experimental methods. Three methods were investigated for the preparation of 4,4-dimethoxy-BODIPYs bearing electron-donating or electron-withdrawing 8-aryl groups: method A employs refluxing in the presence of NaOMe/MeOH, method B uses AlCl₃ in refluxing dichloromethane followed by addition of methanol as nucleophile, and method C involves activation of the BODIPYs using TMSOTf in refluxing toluene followed by addition of methanol. The yields obtained depend on the method used and the structure of the starting BODIPYs; for example, **1a** and **3a** were most efficiently prepared using method C (98 and 70%, respectively), while **2a** was best prepared by method A (50%). Methods B and C were employed for the synthesis of seven new 4,4-dialkoxy-BODIPYs. 4,4-Dipropargyloxy-BODIPY **1e** reacted under Cu(I)-catalyzed alkyne–azide Huisgen cycloaddition conditions to produce 4,4-bis(1,2,3-triazole)-BODIPY **4** in 78% yield. The substitution of the fluorides for alkoxy groups on the BODIPYs had no significant effect on the absorption and emission wavelengths but altered their fluorescence quantum yields. Among this series of dialkoxy-BODIPYs, the 4,4-dipropargyloxy **1e** and its corresponding bis(1,2,3-triazole) **4** show the largest quantum yields in toluene and THF, respectively.



INTRODUCTION

In the last two decades, 4,4-difluoro-4-bora-3a,4a-diaza-*s*-indacene (known as BODIPY) dyes have become an attractive synthetic target for many chemists because of their numerous useful properties.^{1–3} Their high thermal and photochemical stability, strong absorptions in the visible spectral region, and sharp fluorescence with high quantum yields make them desirable for various applications, particularly as fluorescent labels and sensors.^{3–5} The spectroscopic and photophysical properties of BODIPY dyes can be tuned via the introduction of certain groups and functionalities at the peripheral positions of the dipyrromethene core, allowing for example the preparation of BODIPYs with extended π systems that emit in the near-IR region. On the other hand, functionalization of the BODIPY at the boron center (position 4 of the BODIPY core) has little or no effect on the absorption and emission wavelengths but can be used to increase the Stokes shifts, improve aqueous solubility, and modulate the fluorescence properties, stability, and redox behavior of this type of molecule. Nevertheless, boron functionalization has lagged far behind developments at the carbon atoms in BODIPYs. In particular, substitution of the fluorides with alkoxy or aryloxy groups has led to fluorescent BODIPY systems with improved aqueous solubility and with decreased oxidation and reduction potentials that are promising for applications as biological probes and in the construction of donor–acceptor systems.

Two methods can be employed for the synthesis of 4,4-functionalized BODIPYs: (1) by reaction of dipyrromethenes with functionalized boron compounds and (2) by substitution

of the fluorides of BODIPY.^{6,7} Using the latter methodology, the synthesis of 4,4-dialkyl-, 4,4-diaryl-, and 4,4-dialkynyl-BODIPYs have been reported using Grignard or organolithium reagents, in one or two steps.^{8–16} Relatively milder conditions have been investigated for the preparation of 4,4-dialkoxy- and 4,4-diaryloxy-BODIPYs.^{17–26} For example, both the mono- and dimethoxy (up to 52% yield) BODIPYs were obtained upon refluxing BODIPY **1** in methanol and sodium methoxide for 14 h¹⁸ or by using a microwave reactor at 92 °C for 40 min.¹⁹ A milder method for the preparation of 4,4-disubstituted BODIPYs involves the activation of the B–F bonds with aluminum trichloride, followed by reaction with excess alcohols. These conditions are compatible with several functional groups, including aldehydes, esters, and amines.^{20–25} Various alcohols have been investigated, including methanol, benzyl alcohol, phenol, catechol, polyethylene glycol, and ethanediol, producing the corresponding 4,4-dialkoxy- or 4,4-diaryloxy-BODIPYs, in yields ranging from 20% to quantitative.^{20–25} However, the low yields often reported using this methodology, particularly using phenol,²⁰ catechol,⁷ and polyethylene glycol²⁵ as nucleophiles, in part due to difficult purifications due to the need for using a large excess (ca. 278 equiv) of alcohol, have sparked renewed interest in the development of alternative functionalization strategies. One such strategy involves a two-step reaction using boron trichloride to form a reactive 4,4-dichloro-BODIPY derivative, followed by reaction with

Received: November 25, 2014

alkoxide, phenoxide, Grignard, or organolithium reagents to produce the corresponding 4,4-functionalized BODIPYs.^{26–28} A milder method recently reported involves the substitution of one or both fluorides with acetoxy groups in up to 37% yield, with trimethylsilylacetoxy groups, prepared in situ from TMSCl and acetic acid.²⁹ This methodology has also been used for ¹⁹F radiofluorination of BODIPYs.^{30,31} A similar strategy was previously employed for the synthesis of a 4,4-dicyano-BODIPY using trimethylsilyl cyanide in the presence of BF₃·OEt₂ as catalyst.¹³ Alternatively, activation of the BODIPY using trimethylsilyltrifluoromethanesulfonate (TMSOTf) followed by addition of an alcohol as nucleophile is reported to produce the corresponding 4-monoalkoxy-BODIPYs in 38–70% yields.³² This methodology has also been investigated for boron functionalization in subphthalocyanines;³³ this reaction presumably occurs via an activated triflate–subphthalocyanine intermediate, which is reactive toward nucleophilic attack at the boron atom.

Herein we further develop these boron-functionalization methodologies and extend them to the synthesis of 4,4-dialkoxy-BODIPYs, including seven new 4,4-dialkoxy-BODIPYs. We also investigated the reactivity of 4,4-dipropargyloxy-BODIPY **1e** under Cu(I)-catalyzed alkyne–azide click conditions to produce the first boron-bis(1,2,3-triazole)-functionalized BODIPY. The structural (including six X-ray structures), spectroscopic, and fluorescence properties of all synthesized BODIPYs were investigated and are compared and discussed.

RESULTS AND DISCUSSION

Synthesis. The three 8-aryl BODIPYs **1–3** were prepared using a three-step one-pot procedure, as previously described, from commercially available 2,4-dimethylpyrrole and the corresponding aryl aldehyde.³⁴ Electron-donating methoxy or electron-withdrawing methoxycarbonyl groups were introduced at the 8-phenyl group of BODIPYs **2** and **3**, respectively, to investigate their effect on the boron-substitution reaction.

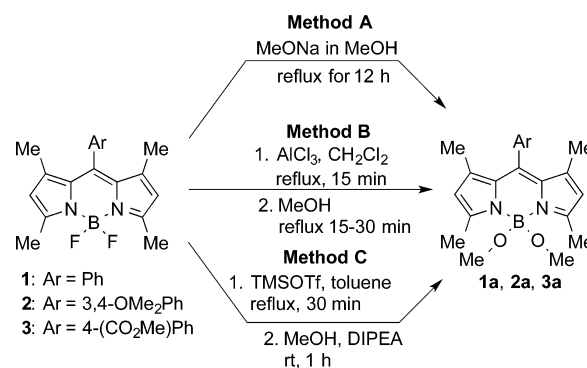
4,4-Dimethoxy-BODIPYs **1a–3a** were obtained in yields ranging from 4% to 98% (Table 1) using the three

Table 1. Isolated Yields of 4,4-Dimethoxy-BODIPYs **1a–3a using Methods A–C**

BODIPY	yield (%)		
	method A	method B	method C
1a	66	52	98
2a	50	11	8
3a	4	58	70

methodologies shown in Scheme 1. Method A employs a one-step reaction using an excess (6 equiv) of sodium methoxide as nucleophile in refluxing methanol, as previously described.¹⁸ Using this methodology, BODIPY **1a** was isolated as the main product in 66% optimized yield, after 12 h of refluxing. The monosubstituted O-BODIPY was an intermediate product under these conditions, as indicated by TLC and as previously observed.⁶ The reaction conditions were applied to BODIPYs **2** and **3** to investigate the applicability of this methodology to functionalized BODIPYs. When BODIPY **2** containing two electron-donating methoxy groups in positions 3 and 4 of the *meso*-phenyl group was subjected to the above reaction conditions, the 4,4-dimethoxy-BODIPY **2a** was produced in 50% yield. On the other hand, BODIPY **3**

Scheme 1. Synthesis of 4,4-Dimethoxy-BODIPYs **1a–3a using Methods A–C**



containing an electron-withdrawing methoxycarbonyl group on the *meso*-phenyl ring produced 4,4-dimethoxy-BODIPY **3a** in only 4% yield, while 53% of starting material was recovered. The presumably lower reactivity of BODIPY **3** under these conditions led us to explore alternative methodologies for the synthesis of 4,4-dialkoxy-BODIPYs (methods B and C in Scheme 1; vide infra). DFT calculations at the B3LYP/6-31+G(d,p) level for evaluation of the natural population analysis (NPA) atomic charges on BODIPYs **1–3** indicate that the charges on the 12-atom BODIPY core are very similar and are not affected by the electron-donating or -withdrawing nature of the 8-aryl group (see the Supporting Information). This is probably due to the large dihedral angles between the 8-aryl and the BODIPY core as a result of 1,7-dimethyl substitution as seen in Figure 1 (vide infra), which prevents electronic communication between the two.

Methods B and C involve a two-step one-pot reaction, in which the BODIPY is first activated, using AlCl₃ or TMSOTf, respectively, followed by reaction with a milder alcohol nucleophile that is compatible with a wider variety of functionalized BODIPYs. In method B (Scheme 1), 2 equiv of AlCl₃ in refluxing dichloromethane was used to activate the BODIPY, followed by addition of a large excess of alcohol (278 equiv), as originally reported.²⁰ On the other hand, the activation of BODIPYs with TMSOTf followed by reaction with an alcohol has only been recently investigated for the synthesis of mono-4-alkoxy-BODIPYs; the reported conditions use 5 equiv of TMSOTf followed by 100 equiv of alcohol and 10 equiv of DIPEA.³² We modified this method and extended it to the preparation of 4,4-dialkoxy-BODIPYs, inspired by a procedure reported for boron functionalization of subphthalocyanines.³³ The optimized procedure uses 2.5 equiv (rather than 5 equiv) of TMSOTf in toluene, followed by addition of 5 equiv (rather than 100 equiv) of alcohol and 5 equiv of DIPEA (method C, Scheme 1); the smaller amount of nucleophile used in this procedure facilitates the purification and isolation of the products. Under these conditions, BODIPY **1a** was produced in 52% (method B) and 98% yields (method C), BODIPY **2a** in 11% (method B) and 8% yields (method C), and BODIPY **3a** in 58% (method B) and 70% yields (method C) (Table 1). Therefore, the newly developed method C produced BODIPYs **1a** and **3a** in the highest yields of the three methods investigated, providing an alternative synthetic route to this type of compound.

The wide range of yields (4–98%) obtained for BODIPYs **1a–3a** under the three methodologies motivated us to investigate the intermediates formed upon fluoride dissociation

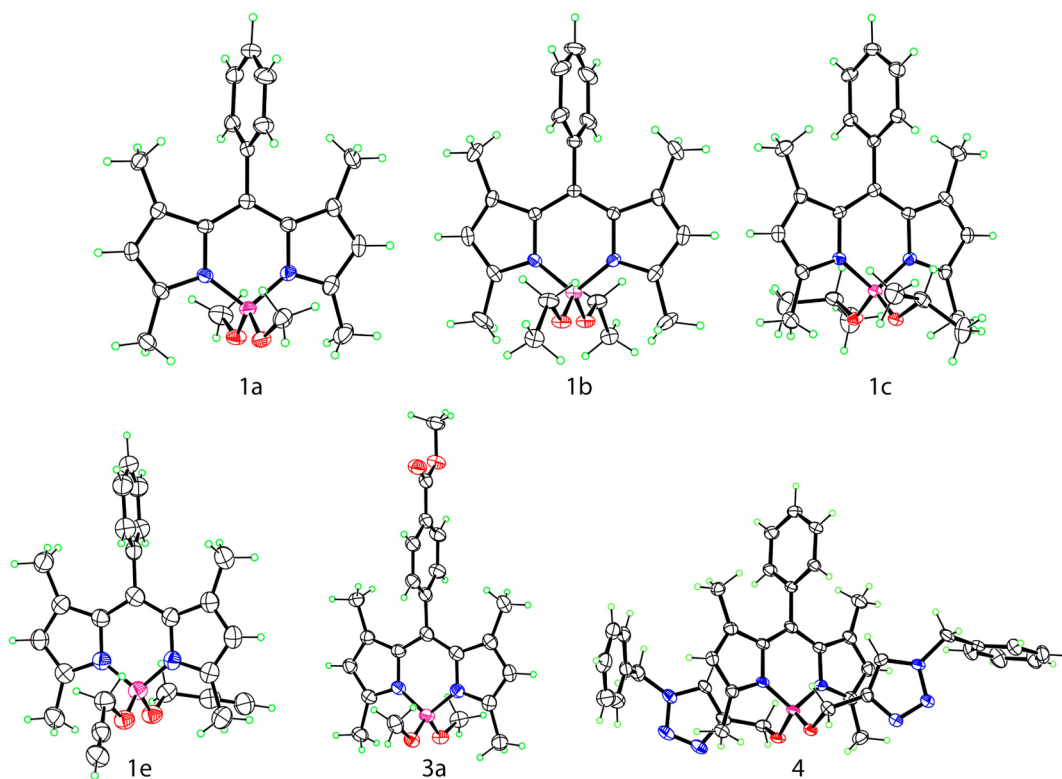
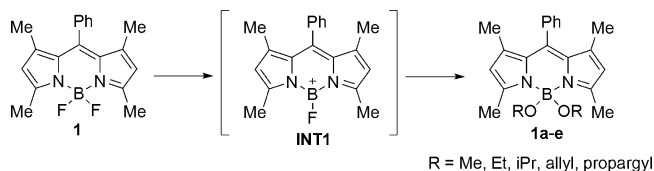


Figure 1. Molecular structures of BODIPYs **1a–c**, **3a**, and **4** from X-ray crystal structure analysis, with 50% probability ellipsoids. Only one of the independent molecules is shown for those structures with $Z' > 1$.

from the BODIPY under each of the reaction conditions, using computational modeling. These substitution reactions likely proceed via formation of the boronium cation intermediate INT1 (Scheme 2); such boronium cations have been previously

Scheme 2. Boronium Intermediate INT1 and BODIPYs **1a–e** Formed using Methods B and C



isolated and characterized by ^{19}F NMR and X-ray crystallography.³⁵ Using DFT modeling, the Gibbs free energies for the formation of INT1 from BODIPY **1** were calculated, and the results obtained are shown in Table 2. The compounds were modeled in methanol for method A, dichloromethane in method B, and toluene in method C. As expected, the dissociation of fluoride ion from BODIPY **1** requires the least amount of energy in methanol (37 kcal/mol), followed by

Table 2. Calculated ΔG Energies for the Formation of INT1 via Methods A–C

method	modeled solvent	anion	ΔG (kcal/mol)
A	CH_3OH	F^-	37
B	CH_2Cl_2	F^-	56
B	CH_2Cl_2	AlCl_3F^-	–22
C	PhCH_3	F^-	92
C	PhCH_3	OTf^-	25

dichloromethane (56 kcal/mol), and it is the hardest to achieve in toluene (92 kcal/mol). This tendency is apparently due to the relative dielectric permittivities of the three solvents: 32.6 for methanol, 8.93 for dichloromethane, and 2.37 for toluene. On the basis of these values, it is likely that the direct dissociation of fluoride ion from BODIPY **1** occurs in method A, since the reaction involves reflux in methanol at ca. 70–75 °C, which allows the reaction barrier to be overcome for the formation of INT1. However, this is not the case in method B, since 56 kcal/mol would need to be overcome. Our calculations indicate that the Lewis acid AlCl_3 significantly stabilizes the boronium cation INT1 due to the formation of the counterion AlCl_3F^- . This is in agreement with the milder conditions required for this reaction. Moreover, our calculations suggest that the reaction could occur at lower temperature. Indeed, performing the reaction entirely at room temperature resulted in the formation of BODIPY **1a**, albeit in lower yield (44 vs 52%) after 12 h. In the case of method C, the abstraction of fluoride likely leads to the formation of INT1 along with triflate anion and trimethylsilyl fluoride; the potential energy barrier of 25 kcal/mol for this reaction can be easily overcome under the conditions of reflux in toluene. Indeed, such a boronium species bearing a triflate ligand has been previously characterized by NMR and X-ray crystallography.³⁶ Moreover, our calculations also suggest similar Gibbs free energies and stabilities for INT1 from all starting BODIPYs **1–3** (ΔG values are 37.4 kcal/mol for **1**, 37.5 kcal/mol for **2**, and 38.7 kcal/mol for **3** following method A, within 1 kcal/mol calculation error).

While for method A the formation of INT1 with a fluoride ion is most likely the rate-determining step, this is not the case for method B. Detailed mechanistic analyses are currently underway³⁷ and will be published elsewhere. In brief, it appears that deprotonation of the alcohol following nucleophilic attack

on boron is the rate-determining step in method B, which also partially explains the need for a large excess of nucleophile in this case. In method C, the use of DMAP in place of DIPEA significantly lowered the yield of BODIPY **1a**, probably due to chelation of DMAP to the boron atom, as previously observed.^{30,31,35,36} The reaction yields were also affected by the temperature and solvent used; when the reaction was performed at room temperature, BODIPY **1a** was isolated in 50% (in toluene), 25% (in dichloromethane), and 29% yields (in chloroform) and it was not formed at all (only starting BODIPY **1** was recovered) when THF was used as the solvent. In some cases, unreacted BODIPY **1** and the mono-4-methoxy-BODIPY were also isolated as side products, in ca. 20 and 17% yields, respectively, when the reaction was performed at room temperature for 2 h in toluene or dichloromethane or overnight in chloroform.

The milder methods B and C were employed for the synthesis of new 4,4-dialkoxy-BODIPYs **1b–e**, as shown in Scheme 2. The isolated yields obtained for the targeted BODIPYs are given in Table 3. While method B gave moderate

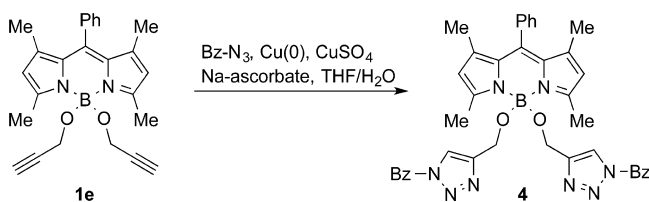
Table 3. Isolated Yields of 4,4-Dimethoxy-BODIPYs **1a–e using Methods B and C**

BODIPY	R	yield (%)	
		method B	method C
1a	Me	52	98
1b	Et	64	18
1c	ⁱ Pr	26	0
1d	allyl	57	30
1e	propargyl	52	40

yields (26–64%) for all targeted BODIPYs, method C was highly sensitive to the bulkiness of the alcohol, likely as a result of the close proximity of the triflate anion to the boron center.³⁷ Indeed, no product was formed when isopropyl alcohol was used as the nucleophile under method C, and the steric demands of the *tert*-butyl alcohol/*tert*-butoxide system has resulted in an effective strategy for BODIPY deboronation.¹⁹ In the case of BODIPY **1b**, the yield could be increased to up 37% when a greater excess of nucleophile was used; the mono-4-ethoxy-BODIPY was also isolated in 20% yield under these conditions. Our results show that consideration of the structures of the starting BODIPY and the nucleophile are needed prior to selection of the methodology, leading to the highest yield of the targeted 4,4-dialkoxy-BODIPYs.

Further derivatization of the 4,4-dipropargyloxy-BODIPY **1e** using click conditions previously investigated for the conjugation of alkyne-functionalized BODIPYs with carbohydrate³⁸ and folate³⁹ moieties was performed (Scheme 3), to demonstrate the tolerance of the 4-propargyloxy groups under the Cu(I)-catalyzed Huisgen cycloaddition conditions. The 4,4-bis(*N*-benzyl-1,2,3-triazole)-BODIPY **4** was formed in 78%

Scheme 3. Click Reaction of BODIPY **1e**



yield from **1e**, using in situ generated copper(I) catalyst from copper(0) and copper(II), in the presence of sodium ascorbate and benzyl azide in aqueous THF. To our knowledge, this is the first report of a click cycloaddition reaction performed on a BODIPY boron functionalized with an alkyne group.

Structural Characterization. All BODIPYs were characterized by ¹H, ¹³C, and ¹¹B NMR, HRMS, UV–vis, and fluorescence and in the case of **1a–c**, **3a**, and **4** also by X-ray crystallography (see Table 4, Figure 1, and the Supporting

Table 4. Calculated Relative Gibbs Free Energies, HOMO and LUMO Energies, and HOMO–LUMO Gap in THF for the Symmetric (1a–e**, **4**) and Unsymmetric (**1a'–e'**, **4'**) BODIPY Conformers**

BODIPY	HOMO (au)	LUMO (au)	gap (eV)	ΔG (kcal/mol)
1a	−0.20599	−0.09520	3.01	0
1a'	−0.2044	−0.09280	3.04	6.76
1b	−0.20542	−0.09440	3.02	0
1b'	−0.20393	−0.09245	3.03	8.39
1c	−0.20548	−0.09436	3.02	0
1c'	−0.20315	−0.09117	3.05	9.92
1d	−0.20694	−0.09608	3.02	0
1d'	−0.20143	−0.09077	3.01	7.82
1e	−0.21009	−0.09941	3.01	0
1e'	−0.20776	−0.09635	3.03	7.45
4	−0.20686	−0.09602	3.02	0
4'	−0.20778	−0.09638	3.03	6.55

Information). The ¹¹B NMR spectra clearly indicated the formation of the targeted 4,4-dialkoxy-BODIPY, via the disappearance of the triplet due to the BF₂ (at ca. 0.6 ppm) and appearance of the singlet attributed to B(OR)₂ at ca. 2 ppm. In the case of **4**, the ¹H NMR clearly indicated the formation of the 1,2,3-triazoles with two singlets at 7.50 and 5.43 ppm for the triazole and benzyl CH₂ protons, respectively.

Crystals suitable for X-ray analysis were grown from slow diffusion of hexane in dichloromethane (for **1a–c** and **4**), acetone (for **1e**), and acetone (for **3a**). The structures, shown in Figure 1, all have at least approximate 2-fold symmetry. BODIPY **1b** has crystallographic C₂ symmetry, and BODIPY **1a** has one molecule on a 2-fold axis and another in a general position. The central six-membered C₃N₂B rings of all five compounds deviate little from planarity, with respective mean and maximum deviations of 0.021 and 0.057 Å for **1a**, 0.024 and 0.037 Å for **1b**, 0.003 and 0.005 Å for **1c**, 0.008 and 0.021 Å for **1e**, 0.035 and 0.075 Å for **3a**, and 0.014 and 0.032 Å for **4**. In all cases, the phenyl plane forms a large dihedral angle with the best plane of the C₉N₂B BODIPY core; these dihedral angles are 84.2 and 83.8° (two independent molecules) for **1a**, 86.5° for **1b**, 84.7° for **1c**, 79.8 and 82.1° (two independent molecules) for **1e**, 84.0 and 84.6° (two independent molecules) for **3a**, and 78.9 and 79.1° (two independent molecules) for **4**. The coordination of the boron atoms is tetrahedral, and 18 B–O bond distances over the six compounds have lengths in the range 1.420(4)–1.444(5) Å, with an average value of 1.432 Å. These distances are in good agreement with those in the *p*-iodophenyl analogue of BODIPY **1a**: 1.420(4) and 1.437(3) Å.²⁰ As in that compound, the conformations of the B–OR groups in all six compounds have the α-C atoms of both alkyl groups folded symmetrically toward the BODIPY core.

The geometries of BODIPYs **1a–e** and **4** were also optimized computationally. In agreement with the X-ray data,

the results showed a nearly tetrahedral geometry around the boron centers and the 8-aryl groups oriented nearly perpendicular to the BODIPY plane. The computational optimization of the structures also revealed the existence of two conformers for all BODIPYs. The most stable conformer is symmetric, with the two B–OR groups symmetrically positioned on both sides of the BODIPY plane (see Figure 2a for **1a**) and the other has the B(OR)₂ group tilted sideways

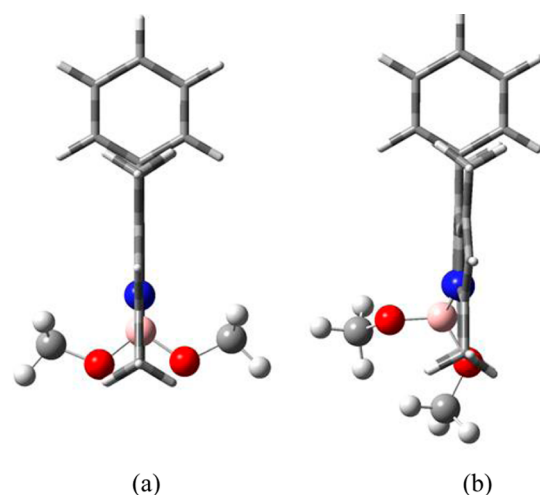


Figure 2. Molecular structures of (a) the symmetric conformer **1a** and (b) the nonsymmetric conformer **1a'** from B3LYP/6-31+G(d,p) optimization.

(shown in Figure 2b for **1a'**). The deviation from planarity for the nonsymmetric conformers of the BODIPYs ranges between 15 and 17° and the relative Gibbs free energies between the two conformers calculated in THF (solvent used for spectroscopic investigations) are given in Table 4. Since the Gibbs energy differences are very small, rapid transition between the two conformers in THF solution freely occurs at room temperature for all BODIPYs. Although only the symmetric conformer is seen in the crystal structures presented in Figure 1, we have previously observed the BODIPY conformer with the boron lying out of the C₃N₂ plane for related BF₂ systems.⁴⁰

Spectroscopic Studies. The spectroscopic properties and fluorescence quantum yields of all BODIPYs in THF and toluene are summarized in Table 5 and shown for three representative BODIPYs in Figure 3 (see also the Supporting Information). The 4,4-dialkoxy-BODIPYs **1a–e**, **2a**, and **3a**

show absorption and emission spectra characteristic for this type of compound, with strong absorption bands ($\log \epsilon = 4.4–5.7$) in the range 501–506 nm and emission bands in the range 505–517 nm in THF and toluene. These results are in agreement with previous studies showing that substitution of fluorides of BODIPY dyes with alkoxy groups produces only minor changes in the absorption and emission wavelengths.^{20,21,25} On the other hand, the bis(1,2,3-triazole)-BODIPY **4** showed a slightly blue shifted absorption (λ_{\max} ca. 495 nm) and the largest Stokes shifts in both solvents. Computational modeling indicates similar HOMO–LUMO gaps for the 4,4-dialkoxy-BODIPYs **1a–e** and **4** (Table 4) in agreement with the observed experimental values. Interestingly, the HOMO–LUMO gaps for the symmetric and the tilted conformers of each compound (Figure 2) are very similar, suggesting that these would not be possible to distinguish spectroscopically.

The fluorescence quantum yields decreased for the 4,4-dimethoxy-BODIPY derivatives **1a–3a** relative to the starting BODIPYs **1–3** in both solvents, likely due to the higher rotational freedom of the methoxy group in comparison with that of fluoride, therefore increasing the amount of energy lost to nonradiative decay to the ground state. This trend was also observed for the 4,4-diethoxy-BODIPY derivative **1b** in THF and for all 4,4-alkoxy-BODIPYs in toluene. However, a similar fluorescence quantum yield in THF was determined for BODIPY **1d** and significant enhancements were observed in the case of BODIPYs **1c,e**, bearing the isopropoxy and propargyloxy groups, respectively, relative to BODIPY **1**. This enhancement of fluorescence has been previously observed for BODIPY derivatives containing isopropoxy and benzyloxy groups.²⁰ The formation of the bis(1,2,3-triazole)-BODIPY resulted in further enhancement of the fluorescence quantum yield in THF but not in toluene. These results suggest that boron functionalization with alkoxy groups tends to decrease the quantum yields in toluene, although enhancement of the quantum yields for certain BODIPYs can be observed in a more polar solvent such as THF. Further derivatization of the propargyloxy groups on boron via click chemistry leads to the formation of a bis(1,2,3-triazole)-BODIPY that shows larger Stokes shifts and enhanced fluorescence quantum yield in THF in comparison with its precursor.

CONCLUSIONS

Three different methods were investigated for the preparation of 4,4-alkoxy-BODIPYs. Method A (NaOMe in refluxing methanol for 12 h) gave the highest yield (50%) of BODIPY

Table 5. Spectroscopic Properties of BODIPYs in THF and Toluene (in Parentheses) at Room Temperature

BODIPY	abs λ_{\max} (nm)	emission λ_{\max} (nm)	Stokes shift (nm)	Φ_f	$\log \epsilon$ (M ⁻¹ cm ⁻¹)
1	501 (504)	505 (511)	4 (7)	0.56 (0.96)	4.96 (5.33)
1a	502 (504)	507 (512)	5 (8)	0.44 (0.73)	4.86 (5.28)
1b	502 (504)	507 (512)	5 (8)	0.46 (0.70)	4.54 (5.24)
1c	501 (504)	505 (509)	4 (5)	0.63 (0.70)	4.70 (5.48)
1d	503 (505)	507 (511)	4 (6)	0.56 (0.57)	4.66 (5.47)
1e	504 (506)	508 (513)	4 (7)	0.62 (0.82)	4.74 (5.04)
2	501 (505)	505 (509)	4 (4)	0.93 (0.87)	5.00 (5.66)
2a	503 (505)	507 (512)	4 (7)	0.42 (0.57)	4.38 (5.06)
3	503 (506)	508 (515)	5 (9)	0.43 (0.51)	4.42 (5.62)
3a	504 (506)	510 (517)	6 (11)	0.31 (0.34)	4.73 (5.48)
4	494 (496)	511 (512)	17 (16)	0.72 (0.56)	4.80 (4.94)

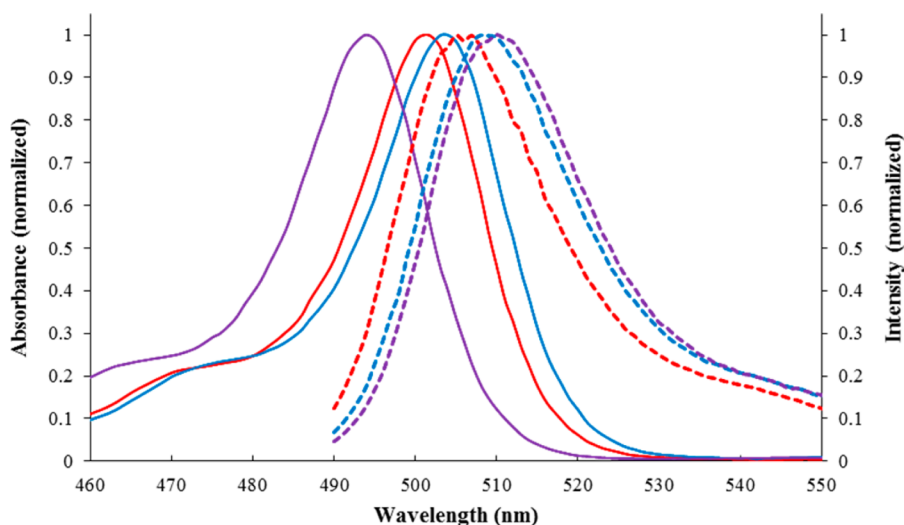


Figure 3. Normalized absorption (full lines) and emission (dashed lines) spectra of BODIPYs **1c** (red), **1e** (blue), and **4** (purple) in THF at room temperature.

2a, bearing an 8-(3,4-dimethoxyphenyl) group. On the other hand, BODIPYs **1a** and **3a** were most efficiently prepared using method C (TMSOTf in refluxing toluene, followed by 5 equiv of methanol and DIPEA), obtained in 98 and 70% yields, respectively. However, for alcohols other than methanol, method C produced lower yields of the targeted 4,4-disubstituted BODIPYs, likely due to steric hindrance caused by the triflate ion. In this case, method B (AlCl₃ in refluxing dichloromethane, followed by a large excess of alcohol) produced the targeted 4,4-dialkoxy-BODIPYs consistently in moderate yields (26–64%). The 4,4-dipropargyloxy-BODIPY was converted to the corresponding bis(1,2,3-triazole)-BODIPY via a Cu(I)-catalyzed Huisgen cycloaddition reaction, demonstrating its stability under these conditions.

The 4,4-dialkoxy-BODIPYs showed absorption and emission spectra similar to those of the parent BODIPY dyes, with only slightly red shifted absorption and emission bands in THF. However, introduction of two large *N*-benzyl-(1,2,3-triazole) groups on boron induced blue-shifted absorption in both THF and toluene. The fluorescence quantum yields of all 4,4-dialkoxy-BODIPYs decreased in toluene, likely due to increased energy loss to nonradiative decay to the ground state. However, in THF the quantum yields were enhanced for the 4,4-diisopropoxy-, 4,4-dipropargyloxy-, and the bis(1,2,3-triazole)-BODIPYs relative to the parent BF₂ dye. Furthermore, the last BODIPY showed the largest Stokes shifts in both solvents.

EXPERIMENTAL SECTION

General Considerations. All of the reagents and solvents were purchased from Sigma-Aldrich without further purification. All reactions were carried out with oven-dried glassware under a dry argon atmosphere. All of the reactions were monitored using Sorbent Technologies 0.2 mm silica gel TLC plates with UV 254 nm indicator. Flash column chromatography was performed using Sorbent Technologies 60 Å silica gel (230–400 mesh). Prep-TLC 60 Å silica gel 20 × 20 cm (210–270 μm) was used. All ¹H, ¹³C, and ¹¹B NMR spectra were collected on an AV-400 spectrometer in deuterated chloroform. The CDCl₃ chemical shifts (δ) are reported in ppm using as reference 7.27 ppm for proton and 77.16 ppm for carbon, and BF₃·OEt₂ was used as reference (δ 0.00) for boron NMR. Coupling constants are reported in hertz (Hz). All of the mass spectra were collected using a Agilent 6210 ESI-TOF mass spectrometer.

General Procedure for Synthesis of BODIPYs 1–3.^{34,41–43}

Aryl aldehyde (9.81 mmol) was suspended in anhydrous CH₂Cl₂ (300 mL). 2,4-Dimethylpyrrole (2.12 mL, 20.6 mmol) was added to the reaction mixture, followed by 6 drops of BF₃·OEt₂. After the mixture was stirred for 48 h and TLC indicated no more aryl aldehyde in the reaction mixture, DDQ (1.113 g, 4.91 mmol) in CH₂Cl₂ was added. After 1.5 h of stirring at room temperature, NEt₃ (10.3 mL, 73.58 mmol) was added and after 1 h BF₃·OEt₂ (12.1 mL, 98.1 mmol) was added. The final mixture was stirred at room temperature for 6 h and then poured into water (50 mL). The organic layer was washed with water (2 × 50 mL). The combined organic layers were dried over anhydrous Na₂SO₄ and concentrated under reduced pressure. The product was purified by silica gel flash column chromatography using mixtures of petroleum ether and dichloromethane for elution.

4,4-Difluoro-8-phenyl-1,3,5,7-tetramethyl-BODIPY (1): obtained as a green-orange solid (20% yield, 650 mg), mp 168–169 °C; ¹H NMR (CDCl₃, 400 MHz) δ 7.47–7.26 (m, 5H), 5.98 (s, 2H), 2.56 (s, 6H), 1.38 (s, 6H); ¹³C NMR (CDCl₃, 100 MHz) δ 155.57, 143.29, 141.87, 135.14, 131.57, 129.26, 129.26, 128.08, 121.34, 14.71, 14.46; ¹¹B NMR (CDCl₃, 128 MHz) δ 0.65 (t, *J* = 33.4 Hz); HRMS (ESI-TOF) *m/z* 324.1718 [M + H]⁺ calculated for C₁₉H₂₀BF₂N₂ 324.1728. These data are in agreement with those previously reported.^{34,41}

4,4-Difluoro-8-(3,4-dimethoxyphenyl)-1,3,5,7-tetramethyl-BODIPY (2): obtained as a red solid (6% yield, 229 mg), mp 182–183 °C; ¹H NMR (CDCl₃, 400 MHz) δ 6.97 (d, *J* = 8.1 Hz, 1H), 6.84 (d, *J* = 8.1 Hz, 1H), 6.80 (s, 1H), 6.00 (s, 2H), 3.96 (s, 3H), 3.86 (s, 3H), 2.56 (s, 6H), 1.49 (s, 6H); ¹³C NMR (CDCl₃, 100 MHz) δ 155.35, 149.80, 149.53, 143.14, 141.59, 131.71, 127.09, 121.12, 120.44, 111.57, 111.10, 56.10, 55.88, 14.53, 14.42; ¹¹B NMR (CDCl₃, 128 MHz) δ 0.62 (t, *J* = 33.0 Hz); HRMS (ESI-TOF) *m/z* 384.1930 [M + H]⁺ calculated for C₂₁H₂₄BF₂N₂O₂ 384.1939. These data are in agreement with those previously reported.^{34,42}

4,4-Difluoro-8-(4-methoxycarbonylphenyl)-1,3,5,7-tetramethyl-BODIPY (3): obtained as a bright red solid (26% yield, 483 mg), mp 181–183 °C; ¹H NMR (CDCl₃, 400 MHz) δ 8.19 (d, *J* = 8.2 Hz, 2H), δ 7.42 (d, *J* = 8.1 Hz, 2H), 5.99 (s, 2H), 3.98 (s, 3H), 2.57 (s, 6H), 1.37 (s, 6H); ¹³C NMR (CDCl₃, 100 MHz) δ 166.58, 156.10, 143.01, 140.35, 139.94, 131.04, 130.94, 130.48, 128.50, 121.62, 52.50, 14.71, 14.61; ¹¹B NMR (CDCl₃, 128 MHz) δ 0.61 (t, *J* = 32.8 Hz); HRMS (ESI-TOF) *m/z* 382.1773 [M + H]⁺ calculated for C₂₁H₂₂BF₂N₂O₂ 382.1752. These data are in agreement with those previously reported.^{34,43}

General Procedure for O-BODIPYs using Method A. In an oven-dried flask, BODIPY (20.0 mg, 0.062 mmol) and NaOMe (21.0 mg, 0.389 mmol) were dissolved in anhydrous methanol (2 mL). The mixture was refluxed for 12 h and then cooled to room temperature.

The reaction mixture was poured into ice water (5.0 mL), extracted with CH_2Cl_2 (3 \times 5.0 mL), washed with brine (1 \times 5.0 mL), and dried over anhydrous Na_2SO_4 . The crude product was concentrated under reduced pressure, and the resulting residue was purified by TLC, using ethyl acetate for elution.

General Procedure for O-BODIPYs using Method B. In an oven-dried flask, BODIPY (20.0 mg, 0.062 mmol) and AlCl_3 (16.4 mg, 0.123 mmol) were dissolved in anhydrous CH_2Cl_2 (5 mL). The mixture was refluxed for 15 min before alcohol (17.15 mmol, 278.0 equiv) was added. The final reaction mixture was refluxed for 15 min. The mixture was cooled to room temperature and then concentrated under reduced pressure. The resulting residue was purified by TLC, using the eluents indicated below.

General Procedure for O-BODIPYs using Method C. In an oven-dried flask, BODIPY (20 mg, 0.06 mmol) and TMSOTf (28.0 μL , 0.154 mmol) were dissolved in anhydrous toluene (5 mL) and the mixture was refluxed for 30 min. The solution was cooled to room temperature, and alcohol (0.308 mmol, 5.0 equiv) was added, followed by DIPEA (27.0 μL , 0.154 mmol, 2.5 equiv). After 1 h of stirring at room temperature, the crude product was concentrated under reduced pressure and purified by TLC, using the eluents indicated below.

4,4-Dimethoxy-8-phenyl-1,3,5,7-tetramethyl-BODIPY (1a). This BODIPY was produced in yields of 66% by method A, 52% by method B, and 98% by method C. The crude product was purified by TLC (eluent EtOAc) to give an orange solid that was recrystallized from 1/1 hexane/dichloromethane: mp 125–130 °C; ^1H NMR (CDCl_3 , 400 MHz) δ 7.50–7.30 (m, 5H), 5.97 (s, 2H), 2.97 (s, 6H), 2.54 (s, 6H), 1.39 (s, 6H); ^{13}C NMR (CDCl_3 , 100 MHz) δ 155.77, 141.71, 141.38, 135.81, 133.01, 129.10, 128.82, 128.35, 121.05, 49.24, 14.70, 14.58; ^{11}B NMR (CDCl_3 , 128 MHz) δ 2.52 (s); HRMS (ESI-TOF) m/z 370.1938 $[\text{M} + \text{Na}]^+$ calculated for $\text{C}_{21}\text{H}_{25}\text{BN}_2\text{NaO}_2$ 370.1923. These data are in agreement with literature data.¹⁸

4,4-Dimethoxy-8-(3,4-dimethoxyphenyl)-1,3,5,7-tetramethyl-BODIPY (2a). This BODIPY was produced in yields of 50% by method A, 11% by method B and 8% by method C. The crude product was purified by TLC (eluent 50:50 hexane/EtOAc) to afford a dark orange/red solid, that was recrystallized from acetone: mp 100–105 °C dec; ^1H NMR (CDCl_3 , 400 MHz) δ 6.97 (d, $J = 8.1$ Hz, 1H), 6.84 (d, $J = 8.1$ Hz, 1H), 6.78 (s, 1H), 5.98 (s, 2H), 3.96 (s, 3H), 3.89 (s, 3H), 2.98 (s, 3H), 2.95 (s, 3H), 2.54 (s, 6H), 1.49 (s, 6H); ^{13}C NMR (CDCl_3 , 100 MHz) δ 155.79, 149.85, 149.53, 141.54, 141.37, 133.30, 128.02, 120.96, 120.86, 111.58, 111.53, 56.31, 56.06, 49.33, 49.26, 14.72; ^{11}B NMR (CDCl_3 , 128 MHz) δ 2.52 (s); HRMS (ESI-TOF) m/z 430.2149 $[\text{M} + \text{Na}]^+$ calculated for $\text{C}_{23}\text{H}_{29}\text{BN}_2\text{NaO}_4$ 430.2136.

4,4-Dimethoxy-8-(4-methoxycarbonylphenyl)-1,3,5,7-tetramethyl-BODIPY (3a). This BODIPY was produced in yields of 4% by method A, 58% by method B, and 70% by method C. The crude product was purified by TLC (eluent EtOAc) to afford an orange solid that was recrystallized from acetone: mp 100–105 °C dec; ^1H NMR (CDCl_3 , 400 MHz) δ 8.19 (d, $J = 8.2$ Hz, 2H), δ 7.42 (d, $J = 8.1$ Hz, 2H), 5.98 (s, 2H), 3.98 (s, 3H), 2.97 (s, 6H), 2.57 (s, 6H), 1.37 (s, 6H); ^{13}C NMR (CDCl_3 , 100 MHz) δ 166.70, 156.34, 141.17, 140.70, 140.21, 132.48, 130.72, 130.37, 128.79, 121.40, 52.50, 49.24, 14.76, 14.73; ^{11}B NMR (CDCl_3 , 128 MHz) δ 2.51 (s); HRMS (ESI-TOF) m/z 428.1992 $[\text{M} + \text{Na}]^+$ calculated for $\text{C}_{23}\text{H}_{27}\text{BN}_2\text{NaO}_4$ 428.1981.

4,4-Diethoxy-8-phenyl-1,3,5,7-tetramethyl-BODIPY (1b). This BODIPY was produced in yields of 64% by method B and 18% by method C. The crude product was purified via TLC (eluent 80/20 hexane/EtOAc) to give an orange solid that was recrystallized from 1/1 hexane/dichloromethane: mp 140–145 °C; ^1H NMR (CDCl_3 , 400 MHz) δ 7.50–7.29 (m, 5H), 5.95 (s, 2H), 3.07 (q, $J = 7.0$ Hz, 4H), 2.58 (s, 6H), 1.38 (s, 6H), 1.07 (t, $J = 7.0$ Hz, 6H); ^{13}C NMR (CDCl_3 , 100 MHz) δ 155.87, 141.61, 141.25, 135.85, 132.84, 129.09, 128.80, 128.37, 121.00, 56.64, 17.83, 14.94, 14.59; ^{11}B NMR (CDCl_3 , 128 MHz) δ 1.82 (s); HRMS (ESI-TOF) m/z 398.2251 $[\text{M} + \text{Na}]^+$ calculated for $\text{C}_{23}\text{H}_{29}\text{BN}_2\text{NaO}_2$ 398.2264.

4,4-Diisopropoxy-8-phenyl-1,3,5,7-tetramethyl-BODIPY (1c). This BODIPY was produced in yields of 26% by method B and 0% by method C. The crude product was purified via TLC (eluent 80/20 Hex/EtOAc) to give an orange solid that was recrystallized from 1/1

hexane/dichloromethane: mp 140–145 °C; ^1H NMR (CDCl_3 , 400 MHz) δ 7.49–7.30 (m, 5H), 5.96 (s, 2H), 3.40–3.34 (septuplet, $J = 6.24$ Hz, 2H), 2.61 (s, 6H), 1.39 (s, 6H), 0.89 (d, $J = 6.08$ Hz, 12H); ^{13}C NMR (CDCl_3 , 100 MHz) δ 156.26, 141.50, 141.42, 135.96, 132.28, 129.06, 128.78, 128.46, 121.16, 63.01, 24.93, 15.76, 14.65; ^{11}B NMR (CDCl_3 , 128 MHz) δ 1.30 (s); HRMS (ESI-TOF) m/z 426.2564 $[\text{M} + \text{Na}]^+$ calculated for $\text{C}_{25}\text{H}_{33}\text{BN}_2\text{NaO}_2$ 426.2575.

4,4-Diallyloxy-8-phenyl-1,3,5,7-tetramethyl-BODIPY (1d). This BODIPY was produced in yields of 57% by method B and 30% by method C. The crude product was purified by TLC (eluent 80/20 hexane/EtOAc) to give an orange solid that was recrystallized from 1/1 hexane/dichloromethane: mp 70–73 °C; ^1H NMR (CDCl_3 , 400 MHz) δ 7.52–7.29 (m, 5H), 5.95 (s, 2H), 5.92–5.82 (m, 2H), 5.15 (d, $J = 1.84$ Hz, 1H), 5.11 (d, $J = 1.88$ Hz, 1H), 4.92 (d, 1H), 4.89 (d, 1H), 3.63 (d, $J = 5.24$ Hz, 4H), 2.56 (s, 6H), 1.38 (s, 6H); ^{13}C NMR (CDCl_3 , 100 MHz) δ 156.06, 141.53, 138.70, 135.77, 132.78, 129.13, 128.85, 128.34, 128.23, 121.18, 113.42, 63.41, 15.03, 14.59; ^{11}B NMR (CDCl_3 , 128 MHz) δ 2.01 (s); HRMS (ESI-TOF) m/z 422.2251 $[\text{M} + \text{Na}]^+$ calculated for $\text{C}_{25}\text{H}_{29}\text{BN}_2\text{NaO}_2$ 422.2254.

4,4-(Diprop-2-yn-1-yloxy)-8-phenyl-1,3,5,7-tetramethyl-BODIPY (1e). This BODIPY was produced in yields of 52% by method B and 40% by method C. The crude product was purified via TLC (eluent 80/20 hexane/EtOAc) to give an orange solid that was recrystallized from 1/1 hexane/dichloromethane: mp 70–73 °C; ^1H NMR (CDCl_3 , 400 MHz) δ 7.49–7.27 (m, 5H), 5.97 (s, 2H), 3.86 (s, 4H), 2.61 (s, 6H), 1.52 (s, 2H), 1.40 (s, 6H); ^{13}C NMR (CDCl_3 , 100 MHz) δ 156.62, 142.22, 141.42, 135.58, 132.79, 129.16, 128.92, 128.26, 121.52, 83.16, 70.83, 49.96, 15.19, 14.58; ^{11}B NMR (CDCl_3 , 128 MHz) δ 1.78 (s); HRMS (ESI-TOF) m/z 418.1938 $[\text{M} + \text{Na}]^+$ calculated for $\text{C}_{25}\text{H}_{25}\text{BN}_2\text{NaO}_2$ 418.1934.

4,4'-(Di-N-benzyl-1,2,3-triazolo-4-methylenoxy)-8-phenyl-1,3,5,7-tetramethyl-BODIPY (4). 4,4-Dipropargyloxy-BODIPY **1e** (15.7 mg, 0.040 mmol, 1.0 equiv) and $\text{Cu}(0)$ (10.1 mg, 0.158 mmol, 4.0 equiv) were dissolved in a mixture of THF and water (8 mL, 3/1) under an inert gas atmosphere. Benzyl azide (0.074 mL, 0.594 mmol, 5.0 equiv) was added dropwise to the reaction mixture. A solution of $\text{CuSO}_4 \cdot 5\text{H}_2\text{O}$ (7.4 mg, 0.030 mmol, 0.75 equiv) and sodium ascorbate (15.7 mg, 0.079 mmol, 2.0 equiv) in THF/water (8 mL, 3/1) was added (after sonication for 30 min) and the reaction mixture was heated for 1.5 h at 70 °C. Once TLC indicated completion of the reaction, the mixture was cooled to room temperature and partitioned between ethyl acetate (30 mL) and water (30 mL). The combined organic layers were dried over Na_2SO_4 and then concentrated under reduced pressure. The crude product was purified via prep-TLC with 20/80 hexane/EtOAc as eluent and recrystallized from 3/1 hexane/dichloromethane to afford the bis(1,2,3-triazole)-BODIPY **4** as a dark orange solid (20.4 mg, 78% yield): ^1H NMR (CDCl_3 , 400 MHz) δ 7.50 (s, 2H), 7.36–7.27 (m, 15H), 5.84 (s, 2H), 5.43 (s, 4H), 4.28 (s, 4H), 2.40 (s, 6H), 1.36 (s, 6H); ^{13}C NMR (CDCl_3 , 100 MHz) δ 155.63, 149.42, 142.17, 135.48, 134.93, 129.21, 129.15, 128.75, 128.35, 128.30, 121.68, 121.48, 56.80, 54.15, 31.06, 29.84, 29.41, 14.96, 14.57; ^{11}B NMR (CDCl_3 , 128 MHz) δ 2.06 (s); HRMS (ESI-TOF) m/z 684.3218 $[\text{M} + \text{Na}]^+$ calculated for $\text{C}_{39}\text{H}_{39}\text{BN}_8\text{NaO}_2$ 684.3229.

Molecular Structures. Crystal structures were determined using low-temperature data from a Bruker Kappa APEX-II DUO diffractometer with either Mo $K\alpha$ or Cu $K\alpha$ radiation. For all structures, H atoms were located from difference maps but constrained in calculated positions during refinement. For **1a**, $Z' = 3/2$, for **1b**, $Z' = 1/2$, and for **1e**, **3a**, and **4**, $Z' = 2$. **3a** was a hemihydrate and a nonmerohedral twin, and **4** was also a nonmerohedral twin. Crystal data for **1a**: $\text{C}_{21}\text{H}_{25}\text{BN}_2\text{O}_2$, $M_r = 348.24$, monoclinic, $a = 20.2592(14)$ Å, $b = 11.2886(8)$ Å, $c = 12.7820(8)$ Å, $\beta = 93.968(3)^\circ$, $U = 2916.2(3)$ Å³, $T = 100$ K, space group $P2_1/c$, $Z = 6$, $D_c = 1.190$ g cm⁻³, $\mu(\text{Cu } K\alpha) = 0.597$ mm⁻¹, 24457 reflections measured, $\theta_{\text{max}} = 68.8^\circ$, 5251 unique reflections ($R_{\text{int}} = 0.032$). The final $R = 0.040$ (4321 $I > 2\sigma(I)$ data), $R_w(F^2) = 0.105$ (all data), CCDC 1035578. Crystal data for **1b**: $\text{C}_{23}\text{H}_{29}\text{BN}_2\text{O}_2$, $M_r = 376.29$, monoclinic, $a = 9.1588(4)$ Å, $b = 11.4850(7)$ Å, $c = 10.1066(4)$ Å, $\beta = 96.860(2)^\circ$, $U = 1055.49(9)$ Å³, $T = 100$ K, space group $P2_1/n$, $Z = 2$, $D_c = 1.184$ g cm⁻³, $\mu(\text{Mo } K\alpha) = 0.075$ mm⁻¹, 33635 reflections measured, $\theta_{\text{max}} = 29.4^\circ$, 3096 unique

reflections ($R_{\text{int}} = 0.045$). The final $R = 0.043$ (2411 $I > 2\sigma(I)$ data), $R_w(F^2) = 0.119$ (all data), CCDC 1035579. Crystal data for **1c**: $C_{25}H_{33}BN_2O_2$, $M_r = 404.34$, monoclinic, $a = 9.0299(11)$ Å, $b = 16.252(2)$ Å, $c = 16.2554(19)$ Å, $\beta = 102.241(7)^\circ$, $U = 2331.3(5)$ Å³, $T = 100$ K, space group $P2_1/c$, $Z = 4$, $D_c = 1.152$ g cm⁻³, $\mu(\text{Mo K}\alpha) = 0.072$ mm⁻¹, 12118 reflections measured, $\theta_{\text{max}} = 25.9^\circ$, 4417 unique reflections ($R_{\text{int}} = 0.091$). The final $R = 0.058$ (2457 $I > 2\sigma(I)$ data), $R_w(F^2) = 0.134$ (all data), CCDC 1035580. Crystal data for **1e**: $C_{25}H_{25}BN_2O_2$, $M_r = 396.28$, monoclinic, $a = 7.9474(8)$, $b = 11.8269(10)$, $c = 45.453(4)$ Å, $\beta = 92.521(6)^\circ$, $U = 4268.2(7)$ Å³, $T = 100$ K, space group $P2_1/n$, $Z = 8$, $D_c = 1.233$ g cm⁻³, $\mu(\text{Cu K}\alpha) = 0.611$ mm⁻¹, 18058 reflections measured, $\theta_{\text{max}} = 67.4^\circ$, 7057 unique reflections ($R_{\text{int}} = 0.045$). The final $R = 0.080$ (5633 $I > 2\sigma(I)$ data), $R_w(F^2) = 0.180$ (all data), CCDC 1035581. Crystal data for **3a**: $C_{23}H_{27}BN_2O_4 \cdot 0.5H_2O$, $M_r = 415.28$, triclinic, $a = 7.6310(6)$ Å, $b = 15.4871(12)$ Å, $c = 19.4805(16)$ Å, $\alpha = 72.585(4)^\circ$, $\beta = 84.215(4)^\circ$, $\gamma = 89.809(4)^\circ$, $U = 2184.7(3)$ Å³, $T = 100$ K, space group $P\bar{1}$, $Z = 4$, $D_c = 1.263$ g cm⁻³, $\mu(\text{Cu K}\alpha) = 0.703$ mm⁻¹, 15119 reflections measured, $\theta_{\text{max}} = 66.9^\circ$, 7555 unique reflections ($R_{\text{int}} = 0.108$). The final $R = 0.067$ (5951 $I > 2\sigma(I)$ data), $R_w(F^2) = 0.196$ (all data), CCDC 1035582. Crystal data for **4**: $C_{39}H_{39}BN_8O_2$, $M_r = 662.59$, triclinic, $a = 11.1659(8)$ Å, $b = 16.0899(12)$ Å, $c = 19.5309(13)$ Å, $\alpha = 90.127(5)^\circ$, $\beta = 92.245(5)^\circ$, $\gamma = 96.332(5)^\circ$, $U = 3484.7(4)$ Å³, $T = 90$ K, space group $P\bar{1}$, $Z = 4$, $D_c = 1.263$ g cm⁻³, $\mu(\text{Cu K}\alpha) = 0.639$ mm⁻¹, 33229 reflections measured, $\theta_{\text{max}} = 67.7^\circ$, 11371 unique reflections ($R_{\text{int}} = 0.062$). The final $R = 0.049$ (8767 $I > 2\sigma(I)$ data), $R_w(F^2) = 0.123$ (all data), CCDC 1051095.

Computational Methods. The reaction mechanism was studied by electronic structure calculations at the B3LYP/6-31+G(d,p) level. The hybrid Becke three-parameter DFT functional was used.^{44,45} The solvent effects were taken into account using the polarized continuum model (PCM).^{46,47} Atomic charges were calculated following the NPA method.⁴⁸ The geometries of all structures were optimized without symmetry constraints. The stationary points on the potential energy surface were confirmed with frequency calculations. All calculations were performed using the Gaussian 09 program package.⁴⁹

Spectroscopic Studies. The photophysical properties of these compounds **1**, **1a–e**, **2**, **2a**, **3**, **3a**, and **4** were determined by preparing a stock solution with a concentration of 5×10^{-5} M that was diluted to the appropriate concentrations for absorbance and emission spectra measurements. All absorption spectra were obtained using a Varian Cary 50 UV/visible spectrophotometer. The optical densities, ϵ , were obtained by preparing solution concentrations between 7.5×10^{-6} and 2.5×10^{-5} M to give λ_{max} values between 0.5 and 1.0. Emission spectra were measured on a PTI QuantaMaster4/2006SE spectrofluorometer with the slit width set at 3 nm. All absorbance and emission spectra were acquired within 3 h of solution preparation, at room temperature. BODIPYs **1–3** were used as standards in THF for calculating the fluorescence quantum yields with excitation at 480 nm (BODIPY **1** $\Phi_f = 0.56$,⁴¹ BODIPY **2** $\Phi_f = 0.93$,³⁴ BODIPY **3** $\Phi_f = 0.43$),³⁴ as previously reported. Rhodamine 6G ($\Phi_f = 0.95$ in EtOH) was used as the reference for BODIPYs **1**, **1a–e**, **2**, **2a**, **3**, **3a**, and **4** in toluene. A spectrophotometric cell with a path length of 10 mm was used.

■ ASSOCIATED CONTENT

● Supporting Information

Figures and CIF files giving X-ray data for **1a–c**, **3a**, and **4** and ¹H, ¹³C, and ¹¹B NMR spectra and normalized absorption and fluorescence spectra of all BODIPYs. This material is available free of charge via the Internet at <http://pubs.acs.org>.

■ AUTHOR INFORMATION

Corresponding Author

*E-mail for M.G.H.V.: vicente@lsu.edu.

Notes

The authors declare no competing financial interest.

■ ACKNOWLEDGMENTS

This work was supported by the National Science Foundation (CHE-1362641). The authors thank the Louisiana Optical Network Initiative (LONI) for the use of their computational facilities and Dr. Svetlana Pakhomova for assistance with the X-ray structure determination for BODIPY **4**.

■ REFERENCES

- (1) Loudet, A.; Burgess, K. *Chem. Rev.* **2007**, *107*, 4891–4932.
- (2) Benstead, M.; Mehl, G. H.; Boyle, R. W. *Tetrahedron* **2011**, *67*, 3573–3601.
- (3) Boens, N.; Leen, V.; Dehaen, W. *Chem. Soc. Rev.* **2012**, *41*, 1130–1172.
- (4) Lavis, L. D.; Raines, R. T. *ACS Chem. Biol.* **2008**, *3*, 142–155.
- (5) Han, J.; Burgess, K. *Chem. Rev.* **2010**, *110*, 2709–2728.
- (6) Ikeda, C.; Maruyama, T.; Nabeshima, T. *Tetrahedron Lett.* **2009**, *50*, 3349–3351.
- (7) Richards, V. J.; Gower, A. L.; Smith, J. E. H. B.; Davis, S. E.; Lahaye, D.; Slater, A. G.; Lewis, W.; Blake, A. J.; Champness, N. R.; Kays, D. L. *Chem. Commun.* **2012**, *48*, 1751–1753.
- (8) Ulrich, G.; Goze, C.; Guardigli, M.; Roda, A.; Ziessel, R. *Angew. Chem., Int. Ed.* **2005**, *44*, 3694–3698.
- (9) Goze, C.; Ulrich, G.; Mallon, L. J.; Allen, B. D.; Harriman, A.; Ziessel, R. *J. Am. Chem. Soc.* **2006**, *128*, 10231–10239.
- (10) Goze, C.; Ulrich, G.; Ziessel, R. *Org. Lett.* **2006**, *8*, 4445–4448.
- (11) Goze, C.; Ulrich, G.; Ziessel, R. *J. Org. Chem.* **2007**, *72*, 313–322.
- (12) Goeb, S.; Ziessel, R. *Org. Lett.* **2007**, *9*, 737–740.
- (13) Li, L.; Nguyen, B.; Burgess, K. *Bioorg. Med. Chem. Lett.* **2008**, *18*, 3112–3116.
- (14) Bonardi, L.; Ulrich, G.; Ziessel, R. *Org. Lett.* **2008**, *10*, 2183–2186.
- (15) Niu, S. L.; Ulrich, G.; Ziessel, R.; Kiss, A.; Renard, P.-Y.; Romieu, A. *Org. Lett.* **2009**, *11*, 2049–2052.
- (16) Ulrich, G.; Goeb, S.; De Nicola, A.; Retaillieu, P.; Ziessel, R. *J. Org. Chem.* **2011**, *76*, 4489–4505.
- (17) Kim, H.; Burghart, A.; Welch, M. B.; Reibenspies, J.; Burgess, K. *Chem. Commun.* **1999**, 1889–1890.
- (18) Gabe, Y.; Ueno, T.; Urano, Y.; Kojima, H.; Nagano, T. *Anal. Bioanal. Chem.* **2006**, *386*, 621–626.
- (19) Smithen, D. A.; Baker, A. E. G.; Offman, M.; Crawford, S. M.; Cameron, T. S.; Thompson, A. *J. Org. Chem.* **2012**, *77*, 3439–3453.
- (20) Tahtaoui, C.; Thomas, C.; Rohmer, F.; Klotz, P.; Dupontail, G.; Mély, Y.; Bonnet, D.; Hibert, M. *J. Org. Chem.* **2007**, *72*, 269–272.
- (21) Tokoro, Y.; Nagai, A.; Chujo, Y. *Tetrahedron Lett.* **2010**, *51*, 3451–3454.
- (22) Wijesinghe, C. A.; El-Khouly, M. E.; Subbaiyan, N. K.; Supur, M.; Zandler, M. E.; Ohkulo, K.; Fukuzumi, S.; D'Souza, F. *Chem. - Eur. J.* **2011**, *17*, 3147–3156.
- (23) Deniz, E.; Battal, M.; Cusido, J.; Sortino, S.; Raymo, F. M. *Phys. Chem. Chem. Phys.* **2012**, *14*, 10300–10307.
- (24) Brizet, B.; Eggenspieler, A.; Gros, C. P.; Barbe, J.-M.; Goze, C.; Denat, F.; Harvey, P. D. *J. Org. Chem.* **2012**, *77*, 3646–3650.
- (25) Brizet, B.; Bernhard, C.; Volkova, Y.; Rousselin, Y.; Harvey, P. D.; Goze, C.; Denat, F. *Org. Biomol. Chem.* **2013**, *11*, 7729–7737.
- (26) Lundrigan, T.; Crawford, S. M.; Cameron, S.; Thompson, A. *Chem. Commun.* **2012**, *48*, 1003–1005.
- (27) Lundrigan, T.; Thompson, A. *J. Org. Chem.* **2013**, *78*, 757–761.
- (28) Groves, B. R.; Crawford, S. M.; Lundrigan, T.; Matta, C. F.; Sowlati-Hashjin, S.; Thompson, A. *Chem. Commun.* **2013**, *49*, 816–818.
- (29) Jiang, X.; Zhang, J.; Furuyama, T.; Zhao, W. *Org. Lett.* **2012**, *14*, 248–251.
- (30) Hendricks, J. A.; Keliher, E. J.; Wan, D.; Hilderbrand, S. A.; Weissleder, R.; Mazitschek, R. *Angew. Chem., Int. Ed.* **2012**, *51*, 4603–4606.
- (31) Brizet, B.; Goncalves, V.; Bernhard, C.; Harvey, P. D.; Denat, F.; Goze, C. *Chem. - Eur. J.* **2014**, *20*, 12933–12944.

- (32) Courtis, A. M.; Santos, S. A.; Guan, Y.; Hendricks, J. A.; Ghosh, B.; Szantai-Kis, D. M.; Reis, S. A.; Shah, J. V.; Mazitschek, R. *Bioconjugate Chem.* **2014**, *25*, 1043–1051.
- (33) Guilleme, J.; Gonzalez-Rodriguez, D.; Torres, T. *Angew. Chem., Int. Ed.* **2011**, *50*, 3506–3509.
- (34) Gibbs, J. H.; Robins, L. T.; Zhou, Z.; Bobadova-Parvanova, P.; Cottam, M.; McCandless, G. T.; Fronczek, F. R.; Vicente, M. G. H. *Bioorg. Med. Chem.* **2013**, *21*, 5770–5781.
- (35) Bonnier, C.; Piers, W. E.; Parvez, M.; Sorensen, T. S. *Chem. Commun.* **2008**, 4593–4595.
- (36) Hudnall, T. W.; Gabbai, F. P. *Chem. Commun.* **2008**, 4596–4597.
- (37) Hopfinger, M. C.; Nguyen, A. L.; Bobadova-Parvanova, P.; Vicente, M. G. H. *Abstracts of Papers; 247th National Meeting of the American Chemical Society, Dallas, TX; American Chemical Society: Washington, DC, 2014; ORGN-177.*
- (38) Uppal, T.; Bhupathiraju, N. V. S. D. K.; Vicente, M. G. H. *Tetrahedron* **2013**, *69*, 4687–4693.
- (39) Ke, M.-R.; Yeung, S.-L.; Ng, D. K. P.; Fong, W.-P.; Lo, P.-C. *J. Med. Chem.* **2013**, *56*, 8475–8483.
- (40) Wang, H.; Fronczek, F. R.; Vicente, M. G. H.; Smith, K. M. *J. Org. Chem.* **2014**, *79*, 10342–10352.
- (41) Kollmannsberger, M.; Rurack, K.; Resch-Genger, U.; Daub, J. *J. Phys. Chem. A* **1998**, *102*, 10211–10220.
- (42) Wang, J. G.; Hou, Y. J.; Li, C.; Zhang, B. W.; Wang, X. S. *Sens. Actuators, B: Chem.* **2011**, *157*, 586–593.
- (43) Qin, W.; Baruah, M.; De Borggraeve, W. M.; Boens, N. *J. Photochem. Photobiol., A: Chem.* **2006**, *183*, 190–197.
- (44) Becke, A. D. *J. Chem. Phys.* **1993**, *98*, 5648–5652.
- (45) Lee, C.; Yang, W.; Parr, R. G. *Phys. Rev. B* **1988**, *37*, 785–789.
- (46) Miertuš, S.; Scrocco, E.; Tomasi, J. *Chem. Phys.* **1981**, *55*, 117–129.
- (47) Tomasi, J.; Mennucci, B.; Cammi, R. *Chem. Rev.* **2005**, *105*, 2999–3093.
- (48) (a) Foster, J. P.; Weinhold, F. *J. Am. Chem. Soc.* **1980**, *102*, 7211–7218. (b) Reed, A. E.; Curtiss, L. A.; Weinhold, F. *Chem. Rev.* **1988**, *88*, 899–926.
- (49) Frisch, M. J.; Trucks, G. W.; Schlegel, H. B.; Robb, M. A.; Cheeseman, J. R.; Scalmani, G.; Barone, V.; Mennucci, B.; Petersson, G. A.; Nakatsuji, H.; Caricato, M.; Li, X.; Hratchian, H. P.; Izmaylov, A. F.; Bloino, J.; Zheng, G.; Sonnenberg, J. L.; Hada, M.; Ehara, M.; Toyota, K.; Fukuda, R.; Hasegawa, J.; Ishida, M.; Nakajima, T.; Honda, Y.; Kitao, O.; Nakai, H.; Vreven, T.; Montgomery, J. A.; Peralta, J. E.; Ogliaro, F.; Bearpark, M.; Heyd, J. J.; Brothers, E.; Kudin, K. N.; Staroverov, V. N.; Kobayashi, R.; Normand, J.; Raghavachari, K.; Rendell, N.; Burant, J. C.; Iyengar, S. S.; Tomasi, J.; Cossi, M.; Rega, N.; Millam, J. M.; Klene, N.; Knox, J. E.; Cross, J. B.; Bakken, V.; Adamo, C.; Jaramillo, J.; Gomperts, R.; Stratmann, R. E.; Yazyev, O.; Austin, A. J.; Cammi, R.; Pomelli, C.; Ochterski, J. W.; Martin, R. L.; Morokuma, K.; Zakrzewski, V. G.; Voth, G. A.; Salvador, P.; Dannenberg, J. J.; Dapprich, S.; Daniels, A. D.; Farkas, O.; Foresman, J. B.; Ortiz, J. B.; Cioslowski, J.; Fox, D. J. *Gaussian 09; Gaussian, Inc., Wallingford, CT, 2009.*